

## Highly transparent and writable wood all-cellulose hybrid nanostructured paper†

Cite this: *J. Mater. Chem. C*, 2013, **1**, 6191

Received 11th July 2013  
Accepted 13th August 2013

DOI: 10.1039/c3tc31331j

[www.rsc.org/MaterialsC](http://www.rsc.org/MaterialsC)

Paper, as an inexpensive substrate for flexible electronics and energy devices, has garnered great attention because of its abundance, biodegradability, renewability and sustainability. However, the intrinsic opacity and higher roughness of regular paper greatly restricts further applications. One promising method is to use cellulose nanofibers (CNs) to fabricate nanopaper with a high optical transmittance and excellent smoothness, but there are still some challenges facing nanopaper substrates, such as high-energy consumption to extract nanofibers and the time-consuming process to prepare nanopaper. We design a bilayer hybrid paper using unbeaten wood fibers and CNs with a papermaking technique, which achieves a high optical transmittance and superior smoothness while remaining less expensive than nanopaper and useful as a writable surface. The first transparent paper touchscreen with an excellent anti-glare effect in bright environments is demonstrated using our novel transparent and conductive hybrid paper as the flexible electrode.

## Introduction

Printed electronics is an emerging research area gathering significant attention. Many recent advances in the field of printed electronics involve fabricating electronic devices, such as displays, transistors, radio frequency identification (RFID) tags, batteries, sensors and solar cells, on common paper.<sup>1–10</sup> Paper electronics is an attractive solution for low-cost applications since cellulosic paper is renewable, environmentally friendly, scalable, light weight, mechanically flexible and disposable.<sup>8,11,12</sup> There are still many challenges facing paper substrates, however, such as their intrinsic opacity due to light scattering by the air which exists in the micro-size cavities

within the networks of wood fibers and their higher roughness compared to commonly used plastics in printed electronics. The root of the challenges for paper as a substrate for printed electronics is that wood fibers are a hollow and elongated cell of a tree, with a micro-sized width and several millimeters in length, which results in micro-sized pores among the paper and high surface roughness. Several approaches have been applied to produce transparent and smooth paper. Transparent paper produced by (1) immersing good quality paper into sulphuric acid for a few seconds to convert part of the cellulose into an amyloid form, which partly fills the pores among the paper; (2) using highly beaten cellulosic pulp that is prepared by intensely fibrillating the cell wall of wood fibers by mechanical treatment, such as refining or beating; (3) impregnating with a fat, oil, resin, paraffin and so on; and (4) forming a web from a mixture of wood fibers and thermoplastic synthetic fibers followed by hot pressing.<sup>13</sup> The transparency of the paper achieved from the above methods is less than 80% and the surface roughness is still high with sizes of several microns. An intriguing way to overcome the aforementioned problems of paper made of micro-sized fibers is by using CNs to produce nanopaper.<sup>11,14</sup> Reports on nanopaper and its applications have arisen in recent years, mainly focusing on engineered nanostructures based on cellulose for transparent and flexible electronic devices. Nanopaper possesses a high optical transmittance (about 90%), strong tensile strength, a low coefficient of thermal expansion (CTE)<sup>15</sup> and a low surface roughness of several nanometers.<sup>16</sup> These excellent characteristics can be utilized to fabricate nanopaper organic field effect transistors (OFETs),<sup>16</sup> nanopaper organic light-emitting diodes,<sup>12,14,17</sup> conductive transparent paper,<sup>18,19</sup> magnetic nanopaper<sup>20</sup> and nanopaper lithium-ion batteries.<sup>21</sup> CNs still require a costly process to extract them from wood fibers because it requires high energy consumption and nanopaper also requires a time-consuming preparation procedure.<sup>22–27</sup>

In this manuscript, we demonstrate the first novel bilayer structural wood fiber/NFC hybrid paper that fulfils the requirements of a high optical transmittance and superior

<sup>a</sup>Department of Materials Science and Engineering, University of Maryland, College Park 20742, USA. E-mail: [binghu@umd.edu](mailto:binghu@umd.edu)

<sup>b</sup>State Key Laboratory of Pulp and Paper Engineering, South China University of Technology, Guangzhou 510640, Guangdong, P.R. China

† Electronic supplementary information (ESI) available. See DOI: 10.1039/c3tc31331j

‡ Equal contribution.

smoothness for flexible electronics. It is less expensive than nanopaper due to the use of unbeaten wood fibers, it is writable, has tunable haze and exhibits superior smoothness. NFC is a type of CN that is obtained by a chemical pre-treatment and mechanical nanofibrillation of the wood fiber.<sup>24</sup> In our hybrid paper, wood fibers form the backbone of the structure, while NFC fills the spaces to decrease the light scattering that otherwise occurs in regular paper substrates. Compared with nanopaper, hybrid paper has a greater optical haze, lower cost and better shape stability as it is easy to fabricate transparent paper with a thickness of over 40  $\mu\text{m}$ . This highly transparent hybrid paper enables a range of printable optoelectronic devices with excellent flexibility. The first transparent paper touchscreen is demonstrated using our novel transparent and conductive nanostructured paper as the flexible electrode.

## Experimental

### Preparation of the nanofibrillated cellulose

Wood fibers refer to a bleached sulfate softwood pulp (Southern Yellow Pine). NFC was manufactured from wood fibers through TEMPO-oxidization and homogenization. The wood fibers were dispersed in distilled water with a concentration of 1% in which sodium bromide and TEMPO were dissolved (10.0 wt% and 1.6 wt% based on oven-dry pulp, respectively)<sup>16</sup>. To gain a uniform fiber suspension, a Turrax mixer (IKA, RW20 digital) was used to disintegrate the agglomerated fibers. The reaction began by the titration of sodium hypochlorite ( $\text{NaClO}$ , 12 wt%) into the suspension at room temperature and the pH was maintained at 10.5 using sodium hydroxide ( $\text{NaOH}$ , 12 wt%) until all the  $\text{NaClO}$  was consumed. The residual solution was removed by filtration, followed by rinsing several times with distilled water. The clean fibers were then dispersed in distilled water at a concentration of 1 wt% and disintegrated by a high-pressure homogenization procedure with a Microfluidizer processor M110EH (Microfluidics Ind., USA).

### Fabrication of the hybrid paper

A nanofibrillated cellulose (NFC) suspension was prepared by diluting to 0.1 wt% in distilled water and then stirring for 1 h at 700 rpm. To verify whether the total light transmittance of the paper improves with the increase of the content of NFC, here we maintained the weight of the wood fiber within the paper and varied the dosage of NFC to fabricate paper with different transmittance values. The wood fiber (bleached sulfate softwood pulp) was dispersed into the aforementioned NFC suspension and stirred for 10 min to form a uniform dispersion. The formula for the paper preparation is shown in Table S2 in the ESI.† Firstly, a 0.1 wt% NFC suspension (56 g) was filtrated with a Buchner funnel using a 90 mm filter membrane (0.65  $\mu\text{m}$  DVPP, Millipore, U.S.A) to form a wet thin layer that contains little free water. Secondly, a mixture of NFC and wood fiber was then poured into the same Buchner funnel to filter and form a hybrid fiber layer on top of the thin pure NFC layer. At last, the bilayer wet film was carefully placed between filter papers and dried under pressure at room temperature.

## Results and discussion

The cell wall of wood fiber is comprised of millions of oriented microfibrils, each with a diameter of 3–5 nm. A typical wood fiber diameter is larger than 10  $\mu\text{m}$ , with a length larger than 0.5 mm (Fig. S1, Table S1, ESI†). In a regular paper substrate, all the fibers are arranged into a random fibrous network with lots of micro-sized air cavities (Fig. 1a). Since the size of the fibers is much larger than the optical wavelength, incident light will largely scatter. The refractive index is 1.5 for cellulose and 1.0 for air. This large difference between refractive indexes invokes light scattering at the fiber surfaces and manifests as the opacity of paper (Fig. 1a). For paper made of bleached softwood kraft fibers, the specific mass attenuation coefficient is 200–350  $\text{cm}^2 \text{g}^{-1}$  and the specific light absorption coefficient is 1–10  $\text{cm}^2 \text{g}^{-1}$ .<sup>28</sup> Light adsorption is much smaller than scattering in paper substrates.

In our design, NFC with diameters of 5–30 nm is used to fill the voids within the paper and thus, micro-sized pores that cause light scattering are reduced to a nano-size by adding NFC *via* a papermaking method. Consequently, minimal light scattering occurs due to the reduced number of open spaces and a matched refractive index between the effective index of the hybrid paper and air, which allows more light to pass directly through the paper rather than getting scattered (Fig. 1b). This leads to an excellent optical transparency of up to 91.5% (Fig. 1c). Similar structures to decrease the light scattering of

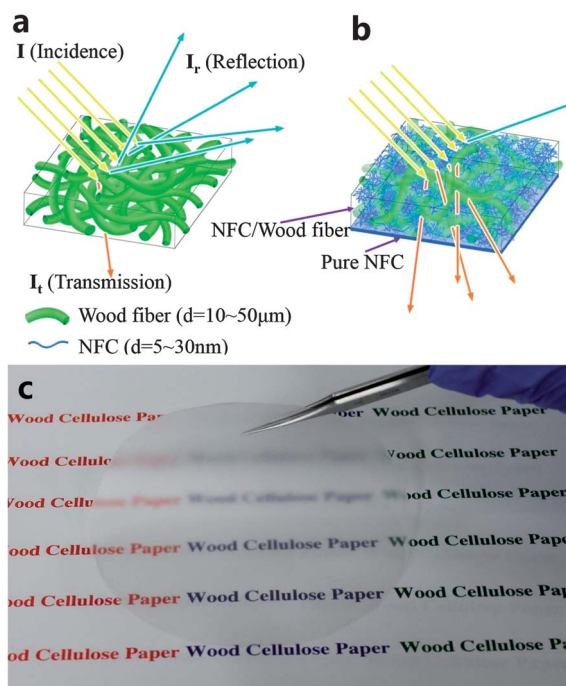


**Fig. 1** (a) Opaque cellulosic paper made of wood fibers. (b) Transparent hybrid paper consisting of two layers: the bottom layer is made of NFC and the top layer is produced by saturating NFC into the pores among the network of wood fibers. The widths of the wood fiber and NFC are 10–50  $\mu\text{m}$  and 5–30 nm, respectively. (c) Photo of the designed all-cellulose hybrid transparent paper with a thickness of 70  $\mu\text{m}$ .

paper substrates have been applied by incorporating other materials, such as resins, oils or starch.<sup>22,29</sup> Compared to previous approaches with two different materials, our hybrid paper (1) consists of only renewable cellulose materials; (2) has a much higher optical transmittance due to the index match of all the components in the composites; (3) is more biocompatible;<sup>30</sup> (4) is potentially more printable for inks for electronics and energy devices; (5) is based on a simple filtration process widely used in the paper industry. In addition to optical transmittance, surface smoothness is also critical for using transparent paper for electronic devices. In our design, a very thin layer of NFC is filtered on the surface of a hybrid structure that ensures nanoscale surface roughness of the hybrid paper.

To execute our design, wood fibers were pre-treated with a TEMPO/NaBr/NaClO oxidation system at a pH of 10 at room temperature and hydroxyl groups at glucose C6 positions are oxidized into carboxyl groups which facilitate fiber swelling and NFC suspension stability.<sup>31–33</sup> TEMPO-oxidized wood fibers are then disintegrated into nanoscale fibers by a Microfluidizer processor (M-110EH). The obtained NFC was mixed with unbeaten wood fibers and then filtered through a nitrocellulose ester filter membrane with a 0.65  $\mu\text{m}$  pore size.<sup>11,33,34</sup> The wet filtered sheet was dried at atmospheric temperature.

Cellulosic papers comprised of various weight percentages of NFC are demonstrated in Fig. 2a. The letters “UMD” gradually become more visible as the content of NFC increases in the hybrid paper, which indicates the paper becomes more transparent. The optical transmittance of the samples was obtained with a Lambda 35 UV-Vis spectrometer (PerkinElmer, USA). The total light transmittances of the various cellulosic papers and polyethylene terephthalate (PET) substrates are illustrated in Fig. 2b, and the basic information of the aforementioned cellulosic papers is listed in Table S3 in the ESI.† Cellulosic paper's transmittance obviously improves as the amount of NFC in the paper increases. When the content of NFC in the paper reaches 60 wt%, the optical transmittance curve nearly overlaps

the curve for PET between wavelengths of 200 nm to 1100 nm. This indicates that our hybrid paper can substitute PET without compromising its performance as a transparent surface. The reason behind this behavior in our samples is that adding more NFC into the cellulosic paper reduces the interfacial area between the regular paper fibers and air by filling the voids in the porous structure. Therefore, more light transmits through the paper instead of being scattered. The hybrid paper with 60 wt% NFC has a total light transmittance of 91.5% at a wavelength of 550 nm, which is similar to the performance of nanopaper with pure NFC.

A detailed study of the optical properties in our hybrid paper is important for evaluating device applications. The haze refers to the visual clarity through a material and may be qualitatively evaluated by the degree of cloudiness observed. The presence of haze may be desirable for some applications due to enhanced light trapping, for example, thin-film solar cells.<sup>35,36</sup> The haze value is defined as the ratio of diffuse transmittance to total transmittance. A PerkinElmer Lambda 35 UV/Vis spectrophotometer is used to accurately measure haze with an integrating sphere. Haze was calculated according to the following experimental equation:

$$\text{Haze (\%)} = \left( \frac{T_4}{T_2} - \frac{T_3}{T_1} \right) \times 100\% \quad (1)$$

where  $T_1$  is the incident light,  $T_2$  is the total light transmitted by the specimen,  $T_3$  is the light scattered by the instrument and  $T_4$  is the light scattered by the instrument and specimen.

Our hybrid paper exhibits a high optical haze in addition to a high transmittance. The haze of cellulosic paper with different weight ratios of NFC and PET plastic is shown in Fig. 2c and Fig. S2 in the ESI.† As the amount of NFC increases in the paper, the haze gradually reduces. This special phenomenon shows that we can design a hybrid paper with a diversity of optical haze factors by altering the weight ratio of wood fiber to NFC, which makes it useful for solar cells as well as anti-glare displays, where optical transmittance and haze are both needed. The optical haze of a transparent hybrid paper depends on the light scattering of the incident light. As the NFC mass ratio increases, the pores inside the hybrid paper decrease, which leads to a decrease of the light scattering. The decrease of light scattering leads to an increase of the forward total transmittance and a decrease of the optical haze.

A scanning electron microscope (SEM) and atomic force microscopy (AFM) were used to observe the morphologies of the NFC and cellulosic paper with different weight ratios. Fig. 3a shows the NFC gel with a concentration of 1% by weight. The NFC gel has a high viscosity and is stable for at least one year. A TEM image of a single NFC is shown in Fig. S3, ESI† and the optical microscopic image in Fig. S4 in the ESI† shows the morphology of the wood fibers. Fig. 3b reveals an AFM image of a freestanding NFC film. The surface morphology of paper with 100% wood fibers is illustrated in Fig. 3c. Fig. 3d and e illustrate the surface morphologies of hybrid paper consisting of 45% and 60% NFC by weight, respectively. The pores on the surface are gradually filled by NFC as the amount of NFC in the hybrid paper increases. When the weight percentage of NFC is 60%, the

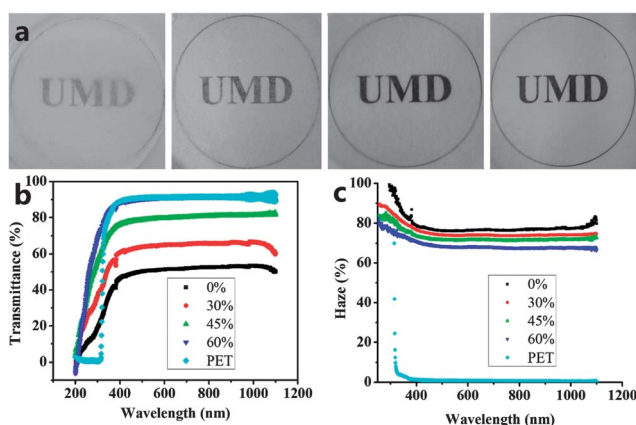


**Fig. 2** Optical properties of cellulosic paper at different weight ratios of NFC to whole paper. (a) The visual appearance of the cellulose paper. The weight ratio of NFC to paper from left to right is 0%, 30%, 45% and 60%. (b) Total light transmittance of the cellulose paper at various weight ratios of NFC. (c) The haze value vs. wavelength for transparent paper with different NFC ratios and PET.

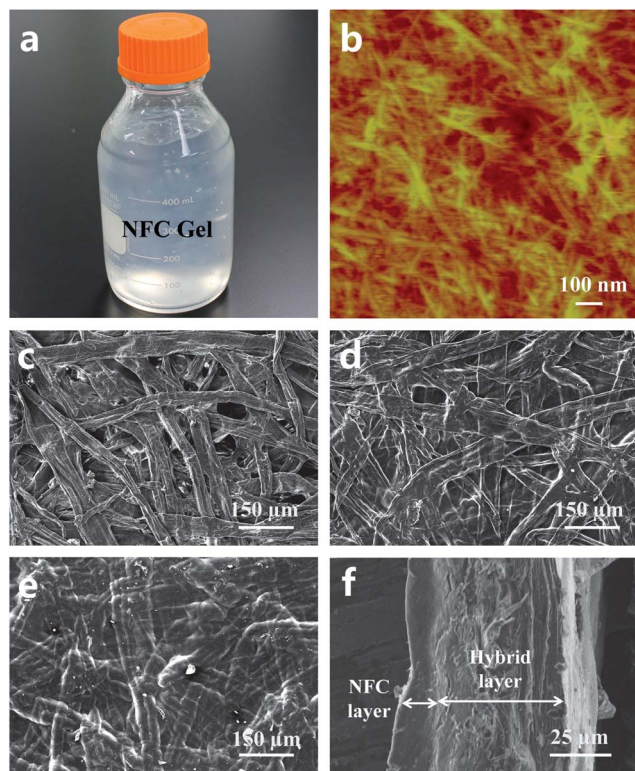


**Fig. 3** NFC gel, AFM image of the NFC and top view SEM images for the rough surface of the cellulosic paper. (a) A digital image of the NFC gel, (b) an AFM image of the NFC. (c) Regular paper without NFC; (d and e) hybrid paper based on NFC and regular fibers with an NFC content of 30% and 45% respectively. (f) SEM cross-section image of the highly transparent nanostructured paper with an hybrid structure, which contains 60% NFC by weight. NFC layer leads to the excellent smoothness of the highly transparent substrates.

open spaces on the surface between the wood fibers are completely filled with NFC from the top-view SEM image. Fig. 3f shows the SEM image of a cross-section of the hybrid paper with 60% NFC by weight, where the bi-layer structure is distinctly observed. The internal micro-sized voids disappear, indicating the NFCs completely fill the spaces among the wood fibers. In our bilayer structural hybrid paper, a thin NFC layer promotes the transparent paper to have a super flat surface, which is required for applications in electronics and optoelectronics.

The transparent paper with a rationally designed structure enables unique functionalities by integrating it with nanomaterials to expand its application beyond information recording and packaging. To fabricate a transparent and conductive paper electrode, 1 mg ml<sup>-1</sup> of carbon nanotubes (CNTs) were dispersed in water with 10 mg ml<sup>-1</sup> of sodium dodecylbenzenesulfonate (SDBS) as a surfactant and applied to the transparent paper. A Meyer rod coating method was used to deposit CNTs on the smoother side of the transparent paper with 60% by weight of NFC, which can be scaled up to an industrial roll-to-roll method. The schematic transverse structure of the CNT-coated transparent hybrid paper is shown in Fig. 4a.

Since the shape stability may affect the fabrication and performance of paper-based electronic devices, serious deformation of the paper should be avoided during the deposition of

functional materials. Shape instability is one of the major challenges to apply electronic devices to previously reported cellulose nanopaper. Transparent hybrid paper consists of a strong interlaced network of micro-sized fibers reinforced by NFC, which forms a structure that enables the hybrid paper to more efficiently resist deformation than nanopaper. The thickness of the transparent hybrid paper fabricated in this study generally exceeds 40 μm owing to the addition of regular fibers with a length weighted average width of 27 μm (Table S1, ESI†). The higher the thickness of a paper, the better the shape stability is. As a result, the hybrid paper attains good shape stability during the aqueous CNTs coating (Fig. 4b). The relationship between the deposited mass of CNTs on the transparent paper and the sheet resistance is illustrated in Fig. S5, ESI†.

One unique property of paper for information technology is its excellent compatibility with pattern generations based on writing or printing processes. To evaluate whether our transparent hybrid paper preserves this property like regular paper, we evaluated the writing with aqueous CNT ink. The word "Writable" is drawn on the relatively rough surface of the hybrid paper using a brush saturated with aqueous CNTs ink and dried

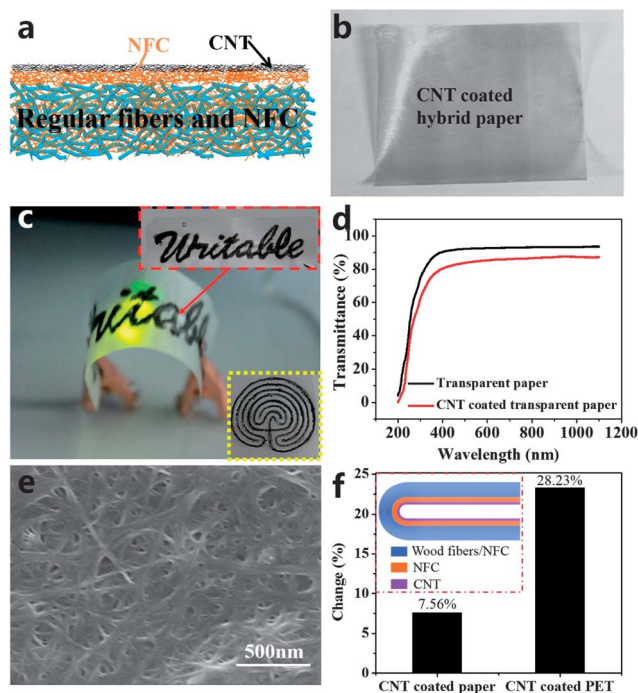


**Fig. 4** Conductive and transparent nanostructured paper. (a) A cross-section schematic structure of the transparent and conductive hybrid paper. (b) Picture of the hybrid paper after CNT coating based on aqueous ink. (c) Image of a highly transparent, writable, flexible and conductive hybrid paper lighting up an LED device. The upper right inset shows the pattern in the hybrid paper drawn by a brusher with CNTs ink, and the insert in the bottom right corner illustrates the circuit drawn by a pen containing CNTs ink. (d) The optical transmittance of the transparent hybrid paper for a touchscreen before and after the CNTs coating. (e) SEM image of CNTs network depositing on the surface of the transparent paper. (f) The sheet resistance change of the CNTs-coated designed hybrid paper and the CNTs-coated PET before and after folding, the schematic in the red dashed rectangle shows the folding direction and degree of the CNTs-coated substrate.

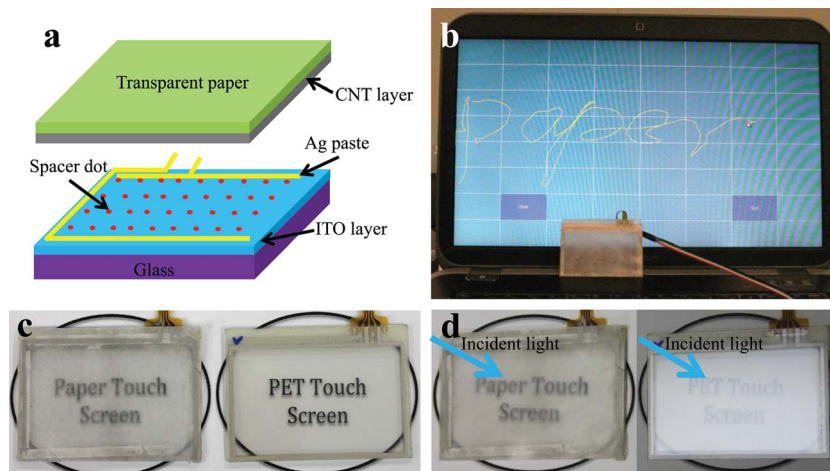


**Fig. 5** (a) A schematic structure of a transparent four-wire touch screen with nanostructured paper. (b) An assembled paper touch screen was used to simulate typical “paper” with the help of eGalaxTouch software from TVI Electronics LLC. (c) Left: a paper touch screen, right: a PET touch screen. (d) Two types of touch screen exposed to sunlight: a paper touch screen without glare (left) and a PET touch screen with great glare (right). All pictures were taken at a similar angle.

under ambient conditions. Then, a green LED light is placed under the curved conductive hybrid paper and connects them with a metal line to form a conductive network. The lighting LED is illuminated by using two 1.5 V batteries. A CNT filled ballpoint pen can be used to draw circuits, which is shown in the bottom right corner of Fig. 4c. Photos of the brush and pen that drew the patterns are pictured in Fig. S6 in the ESI.† The writable, flexible and transparent properties of the hybrid paper may have the potential to fabricate “writable electronics”. Note that the writing process with pens relies on not only the solvent absorption by the substrate, but also the surface roughness. It is anticipated that the roughness of the hybrid paper could be tailored to meet the requirement for both electronics devices and writing processes. Conductive and transparent hybrid paper by incorporating an ultra-thin layer of CNTs is achieved. Fig. 4d shows the optical transmittance of the hybrid paper itself and with the CNTs. The sheet resistance of the CNT coating is around  $700 \text{ Ohm sq}^{-1}$ , which is compatible with the values obtained on a plastic substrate.<sup>37</sup> SEM shows a random network of CNTs uniformly distributed on the hybrid paper surface without the large surface roughness observed in regular paper, which is crucial for electronic devices (Fig. 4e).

Transparent and conductive substrates are extensively used in touch screens, liquid crystal displays (LCDs), organic light-emitting diodes (OLEDs) and solar cells. The mechanical robustness of transparent electrodes is a key factor that influences the lifetime of such devices.<sup>38</sup> Here, we tested the anti-folding ability of the CNT network on PET and designed a hybrid paper by folding the CNT-coated transparent hybrid paper and PET at an angle of  $180^\circ$ . The inset schematic indicates the folding direction of the transparent electrodes. The sheet resistance ( $R_s$ ) of the CNT film was measured before and after folding. The conductive and transparent hybrid paper has a smaller change in  $R_s$  after folding compared to the CNT-coated PET (Fig. 4f). This may be due to the entanglement of wood fibers with high aspect ratios providing an effective strain relief internally.<sup>15</sup> Hybrid paper substrates have a fibrous structure,

fundamentally different to plastic substrates, which is more suitable for foldable electronics.

Such highly conductive paper with good shape stability and a lower cost than nanopaper enables a range of optoelectronic devices impossible to perceive with previous nanopaper. We designed and assembled a four-wire analogue resistive paper touch screen with transparent and conductive hybrid paper as the top transparent electrode. The four-wire analogue resistive touch screen is generally composed of two layers: a PET film and a glass substrate, both coated with a transparent conductor. Here, we demonstrate the first paper four-wire resistive touch screen by replacing the top ITO coated PET film with CNT-coated high transparent paper. Fig. 5a shows the schematic structure of the four-wire resistive paper touch screen used in this study. In our device, silver patterns on the CNT-coated transparent paper were formed by a screen printing method and dried at room temperature. The CNT-coated transparent paper was then used to assemble the paper touch screen. The paper touch screen was tested with the eGalaxTouch software. The word “paper” was written on the touch screen by a stylus pen and successfully displayed on the computer *via* a USB connection (Fig. 5b), which implies the PET may be replaced by the transparent and conductive hybrid paper to fabricate transparent electrodes for electronic devices. The tunable haze and anti-glare effect of the transparent hybrid paper is crucial for many applications, including displays and solar cells. We evaluated the performance of the touch screens under a bright ambient environment. When the PET touch screen and paper touch screen are exposed to light, the touch screen with PET exhibits glare and underneath, the pattern is visibly unclear. The touch screen with the transparent hybrid paper, however, demonstrates high anti-glaring characteristics (Fig. 5d). This is due to two possible effects: (1) the relative rough surface on the top scatters the incident light randomly in different direction instead of a fixed direction, and (2) the optical haze of the hybrid paper. The demonstration of clear visibility in a bright environment is significant for flexible electronics, which could

be one major advantage of transparent nanostructured paper for next-generation green electronics and displays.

## Conclusion

In conclusion, we designed the first, novel hybrid paper consisting of wood fibers as the backbone and NFC as the fillers. Such a hybrid paper has excellent properties, including a high optical transmittance, superior surface roughness, writing capability with inks and good shape stability. Compared with previously transparent nanopaper with pure NFCs, our hybrid paper is much lower cost due to the application of unbeaten wood fibers within the paper and a much faster fabrication process for paper with a similar thickness. A functional touch screen with an excellent anti-glare effect in a bright environment was demonstrated. The economic advantages and enhanced properties of our hybrid paper substrate can reshape the industry for flexible optoelectronic devices, such as touch screen displays and solar cells.

## Acknowledgements

L. Hu acknowledges the financial startup support from the University of Maryland and Air Force Office of Scientific Research (AFOSR) Young Investigator Program. Zhiqiang Fang would like to thank the China Scholarship Council (CSC) for financial support. We acknowledge the support of the Maryland NanoCenter and its NispLab. The NispLab is supported in part by the NSF as a MRSEC (Materials Research Science and Engineering Center) Shared Experimental Facility. In addition, we also acknowledge the Biotechnology Research and Education Program for sharing the Microfluidizer.

## Notes and references

- 1 A. R. Madaria, A. Kumar and C. Zhou, *Nanotechnology*, 2011, **22**, 245201.
- 2 N. Komoda, M. Nogi, K. Suganuma, H. Koga and K. Otsuka, Silver nanowire antenna printed on polymer and paper substrates, presented at *Nanotechnology (IEEE-NANO)*, 2012 12th IEEE Conference on, 20–23 August 2012, pp. 1–5.
- 3 M. C. Barr, J. A. Rowehl, R. R. Lunt, J. Xu, A. Wang, C. M. Boyce, S. G. Im, V. Bulović and K. K. Gleason, *Adv. Mater.*, 2011, **23**, 3500–3505.
- 4 F. Eder, H. Klauk, M. Halik, U. Zschieschang, G. Schmid and C. Dehm, *Appl. Phys. Lett.*, 2004, **84**, 2673–2675.
- 5 A. D. Mazzeo, W. B. Kalb, L. Chan, M. G. Killian, J.-F. Bloch, B. A. Mazzeo and G. M. Whitesides, *Adv. Mater.*, 2012, **24**, 2850–2856.
- 6 L. Nyholm, G. Nyström, A. Mihranyan and M. Strømme, *Adv. Mater.*, 2011, **23**, 3751–3769.
- 7 L. Hu and Y. Cui, *Energy Environ. Sci.*, 2012, **5**, 6423–6435.
- 8 D. Tobjörk and R. Österbacka, *Adv. Mater.*, 2011, **23**, 1935–1961.
- 9 A. Russo, B. Y. Ahn, J. J. Adams, E. B. Duoss, J. T. Bernhard and J. A. Lewis, *Adv. Mater.*, 2011, **23**, 3426–3430.
- 10 Z. Weng, Y. Su, D.-W. Wang, F. Li, J. Du and H.-M. Cheng, *Adv. Energy Mater.*, 2011, **1**, 917–922.
- 11 M. Nogi, S. Iwamoto, A. N. Nakagaito and H. Yano, *Adv. Mater.*, 2009, **21**, 1595–1598.
- 12 Y. Okahisa, A. Yoshida, S. Miyaguchi and H. Yano, *Compos. Sci. Technol.*, 2009, **69**, 1958–1961.
- 13 T. Koike and M. Amano, *U.S. Pat.*, 4,137,046, 30 January 1979.
- 14 M. Nogi and H. Yano, *Adv. Mater.*, 2008, **20**, 1849–1852.
- 15 M. Nogi and H. Yano, *Appl. Phys. Lett.*, 2009, **94**, 233117.
- 16 H. Zhu, L. Hu, J. Cumings, J. Huang, Y. Chen, C. Preston and K. Rohrbach, *ACS Nano*, 2013, **7**, 2106–2113.
- 17 W. Zhang, X. Zhang, C. Lu, Y. Wang and Y. Deng, *J. Phys. Chem. C*, 2012, **116**, 9227–9234.
- 18 G. Chinga-Carrasco, D. Tobjörk and R. Österbacka, *J. Nanopart. Res.*, 2012, **14**, 1–10.
- 19 R. Jung, H.-S. Kim, Y. Kim, S.-M. Kwon, H. S. Lee and H.-J. Jin, *J. Polym. Sci., Part B: Polym. Phys.*, 2008, **46**, 1235–1242.
- 20 R. T. Olsson, M. A. S. Azizi Samir, G. Salazar Alvarez, L. Belova, V. Strom, L. A. Berglund, O. Ikkala, J. Noguez and U. W. Gedde, *Nat. Nanotechnol.*, 2010, **5**, 584–588.
- 21 L. Hu, N. Liu, M. Eskilsson, G. Zheng, J. McDonough, L. Wågberg and Y. Cui, *Nano Energy*, 2013, **2**, 138–145.
- 22 A. N. Nakagaito, M. Nogi and H. Yano, *MRS Bull.*, 2010, **35**, 214–218.
- 23 D. Klemm, F. Kramer, S. Moritz, T. Lindstrom, M. Ankerfors, D. Gray and A. Dorris, *Angew. Chem., Int. Ed.*, 2011, **50**, 5438–5466.
- 24 R. J. Moon, A. Martini, J. Nairn, J. Simonsen and J. Youngblood, *Chem. Soc. Rev.*, 2011, **40**, 3941–3994.
- 25 I. Siro and D. Plackett, *Cellulose*, 2010, **17**, 459–494.
- 26 S. J. Eichhorn, A. Dufresne, M. Aranguren, N. E. Marcovich, J. R. Capadona, S. J. Rowan, C. Weder, W. Thielemans, M. Roman, S. Renneckar, W. Gindl, S. Veigel, J. Keckes, H. Yano, K. Abe, M. Nogi, A. N. Nakagaito, A. Mangalam, J. Simonsen, A. S. Benight, A. Bismarck, L. A. Berglund and T. Peijs, *J. Mater. Sci.*, 2010, **45**, 1–33.
- 27 H. Sehaqui, A. D. Liu, Q. Zhou and L. A. Berglund, *Biomacromolecules*, 2010, **11**, 2195–2198.
- 28 M. A. Hubbe, J. J. Pawlak and A. A. Koukoulas, *BioResources*, 2008, **2**, 627–665.
- 29 B. Konstanze, *The Book and Paper Annual*, 1983, vol. 2, p. 3.
- 30 N. Ferraz, M. Strømme, B. Fellström, S. Pradhan, L. Nyholm and A. Mihranyan, *J. Biomed. Mater. Res., Part A*, 2012, **100**, 2128–2138.
- 31 A. Isogai, T. Saito and H. Fukuzumi, *Nanoscale*, 2011, **3**, 71–85.
- 32 H. Fukuzumi, T. Saito, T. Iwata, Y. Kumamoto and A. Isogai, *Biomacromolecules*, 2008, **10**, 162–165.
- 33 T. Saito, S. Kimura, Y. Nishiyama and A. Isogai, *Biomacromolecules*, 2007, **8**, 2485–2491.
- 34 H. Sehaqui, A. Liu, Q. Zhou and L. A. Berglund, *Biomacromolecules*, 2010, **11**, 2195–2198.
- 35 A. Hongsingthong, T. Krajangsang, I. A. Yunaz, S. Miyajima and M. Konagai, *Appl. Phys. Express*, 2010, **3**, 051102.

- 36 A. V. Shah, M. Vaněček, J. Meier, F. Meillaud, J. Guillet, D. Fischer, C. Droz, X. Niquille, S. Fay, E. Vallat-Sauvain, V. Terrazzoni-Daudrix and J. Bailat, *J. Non-Cryst. Solids*, 2004, **338–340**, 639–645.
- 37 L. Hu, D. S. Hercht and G. Gruner, *Chem. Rev.*, 2010, **10**, 5790–5844.
- 38 D. S. Hecht, D. Thomas, L. Hu, C. Ladous, T. Lam, Y. Park, G. Irvin and P. Drzaic, *J. Soc. Inf. Disp.*, 2009, **17**, 941–946.